DALTON

# Electronic structures and geometries of six-co-ordinate bis(tropolonate)tin hydrocarbyl and chloride complexes. A combined theoretical *ab initio* and gas-phase photoelectron spectroscopy study†

**(the late) Giovanni Bruno, Giuseppe Lanza, Graziella Malandrino and Ignazio Fragalà***

*Dipartimento di Scienze Chimiche, Università di Catania, V. le A Doria 6, 95125 Catania, Italy*

The intriguing relationship between the electronic properties and geometrical structure of six-co-ordinate tin(IV) complexes of general formula $SnL_2(trop)_2$ (L = Cl, $CH_3$, $C_2H_5$ or $C_6H_5$; Htrop = tropolone) has been studied by theoretical *ab initio* calculations and experimental gas-phase UV photoelectron spectroscopy. In agreement with X-ray diffraction data, the theoretical results indicate more stable *cis* arrangements for both $SnCl_2(trop)_2$ and $Sn(CH_3)_2(trop)_2$. The *trans* conformations represent local minima with higher energy (10 and 13 kcal $mol^{-1}$, respectively). The gas-phase UV photoelectron spectra were assigned using *ab initio* data as well as photoelectron data for closely related complexes. The energy and the relative stabilities of molecular orbitals associated with $\sigma_{Sn-L}$ bonds are modulated by the L–Sn–L bond angle and, therefore, the corresponding photoelectron ionization data can be diagnostic of the molecular shape. The almost ubiquitous *cis* geometries of bis-chelate tin(IV) dihalide complexes can be contrasted with the greater flexibility of dimethyl complexes which adopt either *cis* or *trans* structures depending upon the nature of the chelating ligands. This observation can be rationalized in terms of a different involvement of metal orbitals in the metal–ligand bonding.

Since the early discoveries of six-co-ordinate bis-chelate pseudo-octahedral tin(IV) complexes[1–10] great attention has been focused on their stereochemistry. It has been found that the symmetric ligation of bidentate ligands may involve two limiting geometric arrangements: (*i*) the *trans* conformation with a linear $L_2Sn$ moiety and (*ii*) the *cis* arrangement with the $L_2Sn$ bond angle (θ) ≈90°. Several investigations, including X-ray,[11–15] NMR,[16–23] IR,[24] Raman,[25,26] Mössbauer,[27–31] Kerr effect[32,33] and dipole moment[34] measurements, have been reported to date. Despite some discrepancies, today it is well accepted that bis-chelate tin(IV) dihalide complexes adopt slightly distorted *cis* structures.[14] In contrast, dimethyl bis-chelate complexes may adopt either *cis* or *trans* conformations.[14] It has been shown, however, that these molecules are not stereochemically rigid and rapid intramolecular exchange between ligand sites occurs with low energy barriers.[35]

In spite of the aforementioned experimental studies, scarce attention has been paid to the details of the related electronic structures and, in particular, to those factors which, ultimately, govern the molecular arrangement. Single ligand–ligand repulsion models have been used to account for a number of six-co-ordinated organotin molecules.[36] However, electronic effects have never been taken into account. The present contribution reports on a systematic study combining theoretical relativistic effective core potential (RECP) *ab initio* calculations and experimental He I/He II gas-phase photoelectron (PE) measurements of some tin(IV) tropolonate complexes $SnL_2(trop)_2$ (L = Cl, $CH_3$, $C_2H_5$ or $C_6H_5$; Htrop = tropolone, *i.e.* 2-hydroxycyclohepta-2,4,6-trien-1-one) to provide insight into correlations between the geometrical structures and the details of the related metal–ligand electronic interactions.

## Experimental

The complexes were synthesized according to published procedures,[8,9] purified by sublimation *in vacuo* and their purity was checked by NMR spectroscopy.[9,14,22]

† *Non-SI units employed:* eV ≈ 1.60 × $10^{-19}$ J, cal = 4.184 J, eu ≈ 1.60 × $10^{-19}$ C.

Their electron-impact mass spectra‡ have low-intensity molecular-ion peaks, $[M]^+$. No higher-mass peaks were observed in accord with their monomeric nature. All the peaks have isotopic patterns fairly consistent with the expected natural abundance. The most prominent peaks are due to the $[M - L]^+$, $[M - trop]^+$ and $[M - trop - 2L]^+$ fragments. Other, low-intensity peaks, $[M - 2trop - Cl]^+$ and $[M - trop - Cl]^+$, are present in the spectra of $SnCl_2(trop)_2$. In contrast, the most intense peak for the diphenyl complexes is associated with the $[M - trop]^+$ fragment and, in addition, $[M - 2trop - C_6H_5]^+$ and $[Sn(C_6H_5)_3]^+$ are present.

High-resolution PE spectra were measured as described elsewhere.[37] The resolution measured on the helium 1 $s^{-1}$ line was around 25 meV.

## Theoretical Methods

*Ab initio* relativistic effective core potentials[38,39] were employed in the molecular calculations using the restricted Hartree–Fock method for the ground states of $SnCl_2(trop)_2$ and $Sn(CH_3)_2(trop)_2$. The ionization energies (i.e.s) of the higher-lying molecular orbitals (MOs) were also evaluated by calculations of the doublet-state electronic configurations generated upon ionization, using the restricted open Hartree–Fock wavefunctions (ΔSCF). This procedure accounts for the relaxation contribution due to the total reorganization energy. Calculations of the *cis* conformers adopted model ($C_2$ symmetry) geometries taken from X-ray diffraction data.[12–14] In the case of *trans* conformers $C_s$ symmetry was always imposed with the symmetry plane containing the L–Sn–L moiety and bisecting the tropolonate ligands. A series of single-point energy calculations was made for selected intermediate conformations obtained upon rotation about the octahedral '$C_3$' axis. These conformations had L–Sn–L bond angles varying from 95 to 180°, *i.e. cis* to *trans*.

‡ *m*/*z* related to the isotopes $^{120}$Sn and $^{35}$Cl: $SnCl_2(trop)_2$ 432 (8), 397 (100), 311 (79), 276 (10), 241 (68) and 155 (7); $Sn(CH_3)_2(trop)_2$ 392 (1), 377 (100), 271 (95) and 241 (74); $Sn(C_2H_5)_2(trop)_2$ 420 (2), 391 (100), 299 (65) and 241 (73); $Sn(C_6H_5)_2(trop)_2$ 516 (1), 439 (34), 395 (100), 351 (16), 241 (75), 197 (12) and 154 (38%).

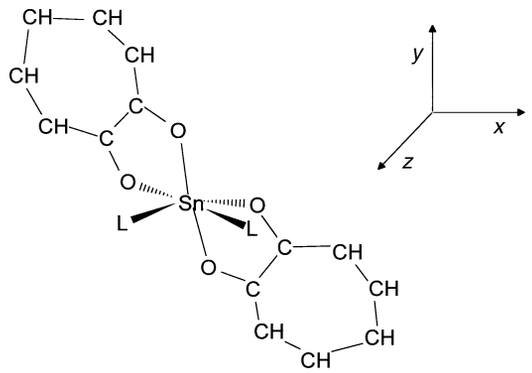


L=Cl, $CH_3$, $C_2H_5$, $C_6H_5$

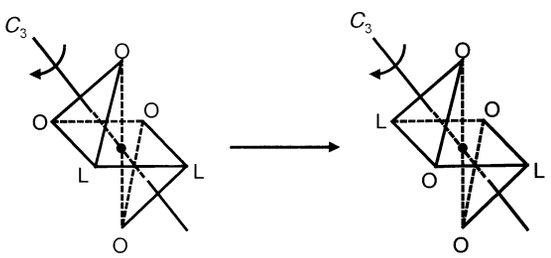


The effective core potentials of Wedt and Hay[38] which explicitly concern the four valence electrons, and a basis set contracted as double ζ with a 'd' polarization function (α = 0.2) were used for the tin atom. For Cl, C and O the effective core potentials and double-ζ basis sets of Stevens *et al.*[39] were used. The standard 31G basis was adopted for H atoms.[40]

All the calculations were performed using HONDO 95.3[41] on IBM ES/9000 and Cray C92 computers.

## Results and Discussion

### Electronic structure of $SnCl_2(trop)_2$ and $Sn(CH_3)_2(trop)_2$

Ground-state eigenvalues and Mulliken populations of the uppermost filled molecular orbitals of the *cis* and *trans* conformers of the dichloride and dimethyl complexes are in Tables 1 and 2, respectively. Related X-ray diffraction studies[12–14] have shown almost symmetrical M–O and C–O bond lengths and, therefore, a local $C_{2v}$ symmetry around the metal centre. The C–C bond length in the O–C–C–O fragment is slightly shorter (≈0.07 Å) than the value quoted for a single C–C bond thus suggesting that it has a minor π character. An obvious consequence is that the electronic structure of the O–C–C–O fragment can be safely described in terms of a α-dicarbonyl system.[42] All the other C–C bond lengths of the $C_7H_5$ ring are similar to those reported for aromatic species (1.38 Å) thus indicating a wide conjugation, within the $C_7H_5$ ring, which involves the two $\pi_{C-O}$ MOs.

In the isolated tropolonate anion ($C_{2v}$) the two in-the-plane carbonyl oxygen lone pairs form in-phase $a_1$ ($n_+$) and out-of-phase $b_1$ ($n_-$) combinations which give rise to two pairs of MOs, either of a and b symmetry in the *cis* conformer ($C_2$) or of a′ and a″ symmetry in the *trans* ($C_s$). They are responsible for the metal–ligand σ bond.[42]

*Ab initio* data for the *cis*-$SnCl_2(trop)_2$ (Table 1) provide evidence that the Sn–trop bonding is mostly σ in nature and involves $n_+$ and $n_-$ based MOs (23a–21b) significantly admixed with the valence 5p metal atomic orbitals. The two $\pi_{C-O}$ orbitals (27b and 27a) are not involved in the bond formation thus remaining similar in energy. The chloride ligands are similarly σ-bonded and involve combinations (MOs 23b and 20a) with 5s, 5p and 4d valence atomic orbitals. The large (2.5 eV) splitting

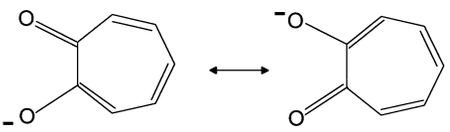


between the two MOs is a consequence of the large 5s and 5p contributions to the 20a. The $\pi_{Cl}$ MOs 25b–24a are almost pure ligand in character and are spread over a narrow (0.47 eV) energy range. A pair of MOs (26a and 26b), very similar in energy and almost totally ligand based, are found in the higher-energy range. They can be related to the symmetry combinations of the more external $\pi_{C-C}$ orbitals of the cycloheptatriene ring.

Upon switching to $Sn(CH_3)_2(trop)_2$ comparable results are found. The metal–ligand σ interactions can be described in terms of tropolonate lone-pair $n_+$ and $n_-$ combinations admixed with the 5p metal orbitals (24b–23a). Compared to the parent $SnCl_2(trop)_2$ these MOs suffer a ≈0.5 eV upward shift, an obvious consequence of the stronger electron-withdrawing effect of the Cl ligands. The Sn–$CH_3$ interactions are σ only in nature with a large metal participation. They are represented by the MOs 26b and 25a which lie more external (≈3 eV) than the $\sigma_{Sn-Cl}$ MOs. The energy splitting between the in- and out-of-phase $\sigma_{Sn-C}$ combinations (≈2 eV) is similar to that found for the $\sigma_{Sn-Cl}$ MOs. A $\sigma_{Sn-C}$ character is also present in the 27b orbital. This is indicative of a four-electron/two-orbital non-bonding interaction involving MOs 27b ($\pi_{C-O}$) and 26b ($\sigma_{Sn-C}$) with a consequent energy splitting of the two $\pi_{C-O}$-related MOs.

The present MO energy sequence is closely reminiscent of that deduced from early PE data for the Tl(trop) complex ($\pi_{C-O} \approx n_+ < \pi_{C_7H_5} \approx n_-$).[42] Relative to the present tin complexes, the lower ionization energy of the $n_+$ MO in the Tl(trop) molecule is due to the strong non-bonding four-electron/two-orbital interaction between the $n_+$ and Tl $6s^2$ based MOs which produces a net destabilization of the $n_+$ MO.[42]

The *ab initio* total charges on the central tin atom, +1.16 (L = Cl) and +1.13 eu (L = $CH_3$), are indicative of an appreciable metal–ligand covalency in both complexes. The electron distribution in the metal atomic orbitals, $5s^{1.47}$ $5p^{0.85}$ $4d^{0.52}$ (L = Cl) and $5s^{1.03}$ $5p^{1.49}$ $4d^{0.35}$ (L = $CH_3$), is similar for the two complexes and indicates a primary role of both the 5s and 5p in the bonding. However, it is notable that the 4d population in the dichloride is greater than in the dimethyl complex. This is the consequence of the large $d_\pi$–$p_\pi$ Sn–Cl interaction.

### Photoelectron spectra

The He I PE spectrum of $SnCl_2(trop)_2$ (Fig. 1 and Table 3) shows four bands (labeled a–d) in the region up to 12.5 eV. The assignment of these features can be safely based on the present calculations (Table 1) as well as on the comparison with PE data for closely related complexes.[42–45] Therefore, the a and b bands are assigned (Table 1) to the two sets of $\pi_{C-O}$ and $\pi_{C_7H_5}$ MOs (27b, 27a and 26b, 26a) both almost totally ligand-based. The calculated energy separation between the baricentre of the two groups (2.06 eV) is similar to the experimental separation (1.78 eV). Their dominant, ligand-based nature is unequivocally supported by the ubiqitous presence of related PE features for all the complexes presently studied. Bands c and d are related to the four $\pi_{Cl}$ and to the antisymmetric $\sigma_{Sn-Cl}$ MOs ionizations (25b–24a and 23b, respectively). The calculated $\Delta E(\pi_{C_7H_5} - \pi_{Cl})$ and $\Delta E(\pi_{Cl} - \sigma_{Sn-Cl})$ differences (0.85 and 0.44 eV) reasonably correlate with the Δi.e. values presently measured between b–c and c–d (0.43 and 0.75 eV). Relative-intensity variations upon switching from the He I to the He II ionizing radiation are also consistent with the assignment. The intensity of band c drops when using He II radiation relative to the remainder and it is well known that the $Cl_{3p}$ cross-section suffers a considerable fall-off with He II,[43,45] due to the occurrence of a Cooper minimum at ≈40 eV incident photon energy.[46] In addition, the associated i.e. value (10.57 eV) lies near the value

**Table 1** *Ab initio* eigenvalues, experimental ionization energies, and Mulliken population analysis for the *cis* and *trans* conformations of $SnCl_2(trop)_2$

| | | | Sn | | | | | | |
|---|---|---|---|---|---|---|---|---|---|
| MO | $-\varepsilon^a$/eV | i.e.[b]/eV | s | p | d | 2 Cl | 4O | 2 $C_7H_5$ | Character |
| *cis* Conformer | | | | | | | | | |
| 27b | 8.65 (8.24) | 8.36 (a) | 0 | 0 | 0 | 2 | 28 | 70 | π(C–O) + π($C_7H_5$) |
| 27a | 8.79 (8.40) | | 0 | 0 | 0 | 1 | 26 | 73 | π(C–O) + π($C_7H_5$) |
| 26b | 10.77 | 10.14 (b) | 0 | 0 | 0 | 2 | 13 | 85 | π($C_7H_5$) |
| 26a | 10.79 | | 0 | 0 | 0 | 3 | 12 | 85 | π($C_7H_5$) |
| 25b | 11.35 | 10.57 (c) | 0 | 1 | 1 | 96 | 0 | 2 | π(Cl) |
| 25a | 11.59 | | 0 | 0 | 2 | 96 | 1 | 1 | π(Cl) |
| 24b | 11.76 | | 0 | 2 | 1 | 89 | 6 | 2 | π(Cl) |
| 24a | 11.82 | | 0 | 2 | 2 | 89 | 3 | 4 | π(Cl) |
| 23b | 12.07 | 11.32 (d) | 0 | 6 | 4 | 53 | 27 | 10 | σ(Sn–Cl) |
| 23a | 12.78 | | 1 | 3 | 2 | 18 | 58 | 18 | $n_-$ |
| 22b | 13.09 | | 0 | 7 | 1 | 17 | 40 | 35 | $n_+$ |
| 22a | 13.43 | | 0 | 3 | 0 | 4 | 66 | 27 | $n_+$ |
| 21b | 13.61 | | 0 | 2 | 0 | 3 | 67 | 28 | $n_-$ |
| 20b | 13.81 | | 0 | 4 | 0 | 10 | 29 | 57 | π($C_7H_5$) |
| 21a | 13.83 | | 1 | 0 | 0 | 0 | 19 | 80 | π($C_7H_5$) |
| 20a | 14.56 | | 8 | 6 | 1 | 33 | 19 | 33 | σ(Sn–Cl) |
| *trans* Conformer | | | | | | | | | |
| 32a′ | 8.79 | | 0 | 0 | 0 | 3 | 28 | 69 | π(C–O) + π($C_7H_5$) |
| 31a′ | 8.81 | | 0 | 0 | 0 | 3 | 28 | 69 | π(C–O) + π($C_7H_5$) |
| 22a″ | 10.59 | | 0 | 0 | 0 | 12 | 14 | 74 | π($C_7H_5$) |
| 26a″ | 10.68 | | 0 | 0 | 0 | 0 | 12 | 88 | π($C_7H_5$) |
| 30a′ | 11.32 | | 0 | 3 | 0 | 91 | 5 | 1 | π(Cl) |
| 25a″ | 11.34 | | 0 | 2 | 0 | 94 | 3 | 1 | π(Cl) |
| 29a′ | 11.35 | | 0 | 0 | 2 | 92 | 1 | 5 | π(Cl) |
| 24a″ | 11.38 | | 0 | 0 | 2 | 84 | 0 | 14 | π(Cl) |
| 28a′ | 11.60 | | 2 | 0 | 5 | 50 | 32 | 11 | $n_+$ + σ(Sn–Cl) |
| 27a′ | 12.80 | | 0 | 16 | 0 | 61 | 4 | 19 | σ(Sn–Cl) |
| 23a″ | 13.05 | | 0 | 0 | 1 | 0 | 90 | 9 | $n_-$ |
| 26a′ | 13.26 | | 0 | 5 | 0 | 5 | 50 | 40 | $n_+$ |
| 22a″ | 13.58 | | 0 | 3 | 0 | 2 | 90 | 5 | $n_-$ |
| 25a′ | 13.79 | | 0 | 0 | 0 | 3 | 15 | 82 | π($C_7H_5$) |
| 24a′ | 13.98 | | 0 | 5 | 0 | 12 | 9 | 74 | π($C_7H_5$) |
| 23a′ | 14.15 | | 7 | 0 | 1 | 15 | 28 | 49 | σ(Sn–Cl) + $n_+$ |

[a] Values in parentheses refer to ΔSCF calculated i.e.s. [b] See Fig. 1 and Table 3.

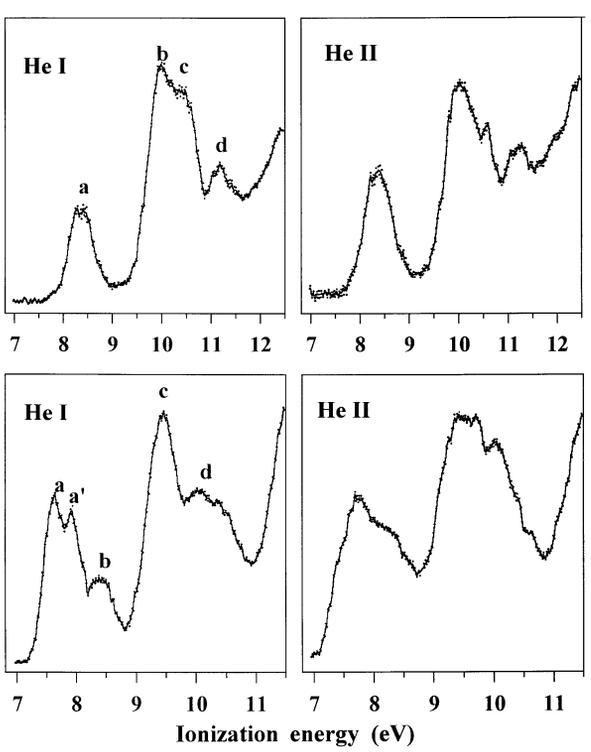


**Fig. 1** Gas-phase He I and He II PE spectra of $SnCl_2(trop)_2$ (upper) (7–12.5 eV) and $Sn(CH_3)_2(trop)_2$ (7–11.5 eV)

for the analogous band in the PE spectrum of $SnCl_2(acac)_2$ (acac = acetylacetonate) (10.47 eV).[43] Note, in this context, that band d does not suffer a similar effect even though the MO 23b contains a sizeable $Cl_{3p}$ character. In fact, the same orbital has considerably $Sn_{5p}$ and $C_{2p}$ mixing and, similarly to what has been reported for $SnCl_3(CH_3)$, $SnCl_2(CH_3)_2$ and $SnCl(CH_3)_3$, these contributions balance the $Cl_{3p}$ effect.[44] This behaviour clearly depends upon the different He I/He II cross-section ratio of various MOs. Within the simpler approximation of the Gelius model,[47] the one-electron cross-section ($\sigma_j$) for the *j*th MO is given by $\sigma_j = \Sigma_{A,i}\, P_{j,i,A}\, \sigma_i^A$. In the present linear combination of atomic orbitals (LCAO)-MO treatment the summation is carried out over contributions of each AO on the different atoms *A* ($\sigma_{iA}$)[46] weighted by a factor ($P_{j,i,A}$) given by the squares of the atomic MO coefficients ($c_{i,j,A}$). In this context, calculated molecular cross-section data indicate a dramatic He II fall-off for Cl-based MOs (95%, MO 25b) relative to tropolonate-based MOs (64%, MO 26b). A moderate He I *vs.* He II intensity reduction is found in the case of MO 23b (78%), in agreement with experiments.

The PE spectra of $Sn(CH_3)_2(trop)_2$ (Fig. 1 and Table 3) appear more structured in the low i.e. region thus consisting of five bands (labelled a, a′, b, c and d) up to 11.5 eV. Similarly to $SnCl_2(trop)_2$, bands a and a′ are related to the ionizations associated with the two external $\pi_{C-O}$ MOs 27b and 27a (Table 2). In contrast with the chloride homologue, they are well resolved in agreement with the theoretical Δi.e. 0.28 eV against 0.14 eV for $SnCl_2(trop)_2$ (Table 1). Band c, in analogy to $SnCl_2(trop)_2$, is related to non-bonding $\pi_{C_7H_5}$ ligand-based

**Table 2** *Ab initio* eigenvalues, experimental ionization energies, and Mulliken population analysis for the *cis* and *trans* conformations of $Sn(CH_3)_2(trop)_2$

| | | | Sn | | | | | | |
|---|---|---|---|---|---|---|---|---|---|
| MO | $-\varepsilon$/eV | i.e.[b]/eV | s | p | d | 2 $CH_3$ | 4O | 2 $C_7H_5$ | Character |
| *cis* conformer | | | | | | | | | |
| 27b | 7.99 (7.60) | 7.63 (a) | 0 | 2 | 1 | 11 | 27 | 59 | $\pi$(C–O) + $\pi(C_7H_5)$ |
| 27a | 8.27 (7.89) | 7.91 (a′) | 0 | 0 | 0 | 0 | 27 | 73 | $\pi$(C–O) + $\pi(C_7H_5)$ |
| 26b | 9.22 | 8.40 (b) | 0 | 17 | 3 | 60 | 8 | 12 | $\sigma(Sn-CH_3)$ |
| 25b | 10.37 | 9.51 (c) | 0 | 0 | 0 | 0 | 15 | 85 | $\pi(C_7H_5)$ |
| 26a | 10.40 | | 0 | 0 | 0 | 0 | 14 | 86 | $\pi(C_7H_5)$ |
| 25a | 11.29 | 10.09 (d) | 8 | 10 | 2 | 37 | 31 | 12 | $\sigma(Sn-CH_3)$ |
| 24b | 12.31 | | 0 | 4 | 0 | 4 | 56 | 36 | $n_+ + \pi(C_7H_5)$ |
| 24a | 12.80 | | 0 | 2 | 0 | 4 | 80 | 14 | $n_-$ |
| 23b | 13.02 | | 0 | 3 | 0 | 2 | 87 | 8 | $n_-$ |
| 23a | 13.21 | | 8 | 0 | 0 | 25 | 31 | 36 | $n_+ + \sigma$(C–H) |
| 22b | 13.22 | | 0 | 0 | 0 | 16 | 16 | 68 | $\pi(C_7H_5)$ |
| 22a | 13.39 | | 0 | 1 | 0 | 7 | 18 | 74 | $\pi(C_7H_5)$ |
| 21b | 13.62 | | 0 | 1 | 0 | 81 | 6 | 12 | $\sigma$(C–H) |
| *trans* conformer | | | | | | | | | |
| 32a′ | 7.99 | | 0 | 2 | 0 | 9 | 30 | 59 | $\pi$(C–O) + $\pi(C_7H_5)$ |
| 31a′ | 8.25 | | 0 | 0 | 0 | 1 | 30 | 69 | $\pi$(C–O) + $\pi(C_7H_5$ |
| 30a′ | 9.67 | | 12 | 0 | 5 | 45 | 30 | 8 | $\sigma(Sn-CH_3)$ |
| 22a″ | 10.24 | | 0 | 0 | 0 | 1 | 15 | 84 | $\pi(C_7H_5)$ |
| 21a″ | 10.26 | | 0 | 0 | 0 | 0 | 15 | 85 | $\pi(C_7H_5)$ |
| 29a′ | 11.68 | | 0 | 27 | 0 | 58 | 0 | 15 | $\sigma(Sn-CH_3)$ |
| 28a′ | 12.46 | | 0 | 3 | 0 | 5 | 55 | 37 | $n_+ + \pi(C_7H_5)$ |
| 20a″ | 12.50 | | 0 | 0 | 0 | 0 | 91 | 9 | $n_-$ |
| 19a″ | 12.87 | | 0 | 2 | 0 | 6 | 87 | 5 | $n_-$ |
| 27a′ | 13.11 | | 2 | 0 | 0 | 18 | 21 | 59 | $\pi(C_7H_5)$ |
| 26a′ | 13.35 | | 6 | 0 | 0 | 14 | 32 | 48 | $n_+ + \pi(C_7H_5)$ |
| 18a″ | 13.40 | | 0 | 0 | 0 | 60 | 25 | 15 | $\sigma$(C–H) |
| 25a′ | 13.43 | | 0 | 2 | 0 | 2 | 13 | 83 | $\pi(C_7H_5)$ |

[a] Values in parentheses refer to ΔSCF calculated i.e.s. [b] See Fig. 1 and Table 3.

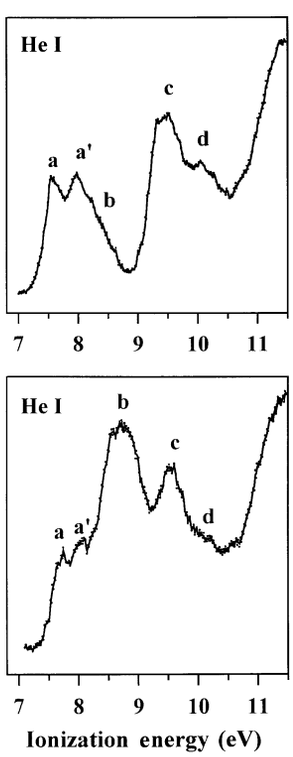


**Fig. 2** Gas-phase He I PE spectra of $Sn(C_2H_5)_2(trop)_2$ (upper) and $Sn(C_6H_5)_2(trop)_2$ in the 7–11.5 eV region

orbitals. The low-intensity features b and d, not present in the spectrum of the parent dichloride, represent ionizations (Table 2) from the out-of-phase (26b) and in-phase (25a) combinations of the $\sigma_{Sn-C}$ MOs, respectively. Finally, the energy separations between the relevant groups of MOs [$\Delta E(\pi_{C-O} - \sigma_{Sn-C}) = 1.09$, $\Delta E(\sigma_{Sn-C} - \pi_{C_7H_5}) = 1.17$ and $\Delta E(\pi_{C_7H_5} - \sigma_{Sn-C}) = 0.90$ eV], correlate reasonably with experimental Δi.e. values inferred from PE data (0.63, 1.11 and 0.58 eV, respectively).

A similar spectrum has been recorded for the $Sn(C_2H_5)_2(trop)_2$ analogue (Fig. 2, Table 3), therefore the same assignment may be proposed. The spectrum of $Sn(C_6H_5)_2(trop)_2$ (Fig. 2 and Table 3) can be similarly assigned using comparative arguments with the mentioned parent complexes as well as with PE data for related molecules (Fig. 3). Note in this context that band b at 8.77 eV, absent for the present related complexes, represents ionizations from the $e_{1g}$-related orbitals of the aromatic ring (9.25 eV for $C_6H_6$).[48]

Finally, the Koopmen's i.e.s for both $SnCl_2(trop)_2$ and $Sn(CH_3)_2(trop)_2$ are slightly overestimated relative to the experimental data due to reorganization (relaxation and correlation) effects upon ionization. The application of simple ΔSCF procedures to account for relaxation effects into the evaluation of uppermost i.e.s gives a very good agreement with experiment for both $SnCl_2(trop)_2$ (8.24 and 8.40 *vs.* 8.36 eV) and $Sn(CH_3)_2(trop)_2$ (7.60 and 7.89 *vs.*7.63 and 7.91 eV) (Tables 1 and 2) even though correlation has not been included. It is, however, generally recognized that ionizations from largely delocalized MOs do not involve large variations of correlation energies.[49]

## Stereochemical implications

To put the present data into perspective, it is relevant to comment on the electronic factors which govern the relative stabilities of *cis vs. trans* conformers. The dependence of the total energy upon variations in the L–Sn–L bond angle (Fig. 4) shows that the geometries of both the dimethyl and dichloride complexes are associated with equilibrium *cis* structures and, in fact, the calculated L–Sn–L bond angles (100 and 108°) are similar to those inferred from X-ray diffraction data (95 and

**Table 3** Relevant PE spectroscopic data (eV) for $SnL_2(trop)_2$ complexes

| Band | $SnCl_2(trop)_2$ | $Sn(CH_3)_2(trop)_2$ | $Sn(C_2H_5)_2(trop)_2$ | $Sn(C_6H_5)_2(trop)_2$ |
|---|---|---|---|---|
| a | 8.36 | 7.63 | 7.52 | 7.76 |
| a′ | | 7.91 | 7.95 | 8.05 |
| b | 10.14 | 8.40 | 8.33 | 8.77 |
| c | 10.57 | 9.51 | 9.45 | 9.61 |
| d | 11.32 | 10.09 | 10.06 | 10.10 |

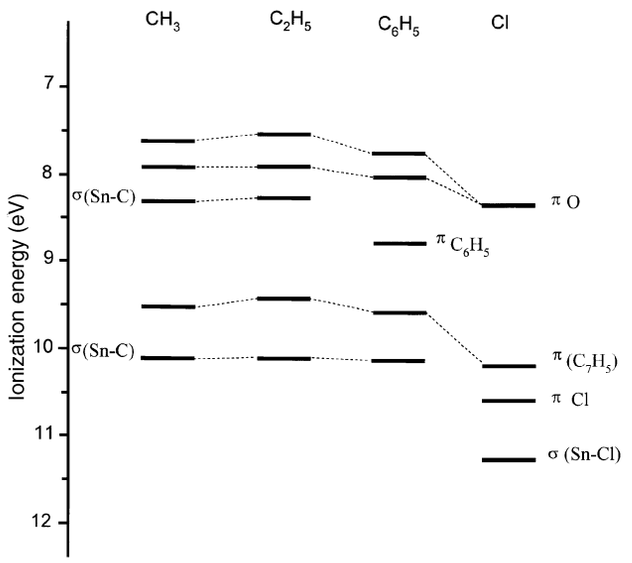


**Fig. 3** Ionization energies of $SnL_2(trop)_2$ (L = Cl, $CH_3$, $C_2H_5$ or $C_6H_5$) complexes

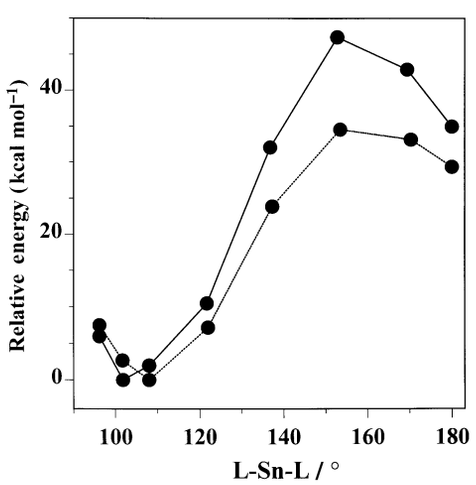


**Fig. 4** Potential-energy curves for $SnCl_2(trop)_2$ (solid line) and $Sn(CH_3)_2(trop)_2$ (dashed line) *versus* the L–Sn–L bond angle

108°).[12–14] Moreover, calculations show local, higher-energy minima [10 kcal $mol^{-1}$, $SnCl_2(trop)_2$ and 13 kcal $mol^{-1}$, $Sn(CH_3)_2(trop)_2$] for *trans* conformations with the *cis–trans* isomerization energy barrier around ≈40 kcal $mol^{-1}$. These values are first-order estimations since geometrical parameters have not been optimized. Note that the geometries with a 180° L–Sn–L bond angle do not have perfectly coplanar tropolonate rings because the L–Sn–O and O–Sn–O bond angles differ from 90°. Therefore, the *cis–trans* energy differences have been evaluated in terms of differences between the *cis* and the $C_s$ geometries (see **Theoretical Methods**).

Comparative arguments, in terms of both eigenvalues and population data, point to sizeable differences only for those MOs which represent the $\sigma_{Sn-Cl}$ and $\sigma_{Sn-C}$ bonds (Tables 1 and 2) upon switching from the *cis* to the *trans* conformers. Thus, in the *trans* conformers, the symmetric combinations of $\sigma_{Sn-L}$ MOs representing the Sn–Cl and the Sn–C bonds, despite the nodal properties, lie higher in energy than the antisymmetric ones. A reversed ordering is observed in the *cis* conformers. Fig. 5 shows the dependence of the energy of the in-phase (25a) and out-of-phase (26b) MOs of $Sn(CH_3)_2(trop)_2$ upon rotation around the '$C_3$' axis. [Very similar behaviour has been noted for MOs 23b and 20a of $SnCl_2(trop)_2$.] The energy of MO 25a increases whilst MO 26b becomes more stable upon linearization of the L–Sn–L angle. This trend is clearly due to diverging overlap integrals involved in the metal–ligand interactions upon changing the L–Sn–L bond angle (Fig. 5). Therefore, in the *cis* conformers favourable overlaps involve combinations of ligand orbitals and either the $5p_z/5s$ (25a) or the $5p_x$ (26b) metal atomic orbitals. Upon linearization ($\theta = 180°$) of the L–Sn–L framework, the interaction involving $5p_z$ acquires some non-bonding character and, therefore, MO 25a becomes less stable. In contrast, orbital 26b is stabilized since there is a greater overlap involving the $5p_x$ metal orbital. Effects due to differential overlaps involving the 5s tin orbital are of minor relevance due to its spherical shape.

Even more important for structural diagnostic purposes, the energy separation between the two mentioned $\sigma_{Sn-L}$ combinations ranges from ≈1 eV in the *trans* conformers to >2 eV in the *cis* (Tables 1 and 2). Therefore, the i.e. values measured from the PE spectra offer a valuable, diagnostic tool for the C–Sn–C or for the Cl–Sn–Cl bond angles. The experimental Δi.e.($\sigma_{Sn-L}$) values measured for both $Sn(CH_3)_2(trop)_2$ and $Sn(C_2H_5)_2(trop)_2$ lie around 2 eV (Figs. 1, 2 and Table 3), thus pointing to *cis* geometries in agreement with other experiments.[12,13,32] Unfortunately only one band is clearly resolved in the spectra of $Sn(C_6H_5)_2(trop)_2$ and $SnCl_2(trop)_2$ with the remainder hidden under broad, unresolved features. Although a quantitative evaluation is not possible, it is noted that the PE spectrum of the dichloride complex possesses a 1.5 eV window beyond the ($\sigma^-_{Sn-Cl}$) ionization and, therefore, the partner $\sigma^+_{Sn-Cl}$ ionization must lie at a higher i.e. As a consequence, the *cis* structure expected is in agreement with other structural characterizations.[14,22]

Relevant insights into the electronic factors which govern the geometry of these complexes can be obtained from the metal atomic contributions to MOs involved in the bonding. In particular, a greater, total metal admixture is found in both the $n_\pm$ ($\sigma_{Sn-O}$) and $\pi_{Sn-Cl}$ MOs of $SnCl_2(trop)_2$ on passing from the *trans* to the *cis* structure (Table 1), hence covalent interactions are favoured in the *cis* geometry. The effects are more evident in $Sn(CH_3)_2(trop)_2$. The total metal contribution to the $n_\pm$ ($\sigma_{Sn-O}$) MO increases in the *cis* conformation (11%, for *trans vs.* 17% for *cis*) whilst the opposite trend is found for the $\sigma_{Sn-C}$ (44% for *trans vs.* 40% for *cis*); the *cis* conformation is, therefore, preferred due to the increased Sn–O interactions over the Sn–C ones.

These results are in good agreement with earlier structural studies on several pseudo-octahedral $SnL_2(chelate\ ligand)_2$ complexes.[14] The *cis* geometry is, therefore, ubiquitous in $SnX_2(chelate\ ligand)_2$ (X = halide)[14] since both Sn–X and Sn–O covalent interactions are favoured. In dimethyl derivatives the equilibrium structures depend upon the relative strengths of the $\sigma_{Sn-C}$ and $\sigma_{Sn-O}$ interactions. As a consequence, *trans* arrangements are found in $Sn(CH_3)_2(acac)_2$, $Sn(CH_3)_2(O_2CCH_3)_2$,

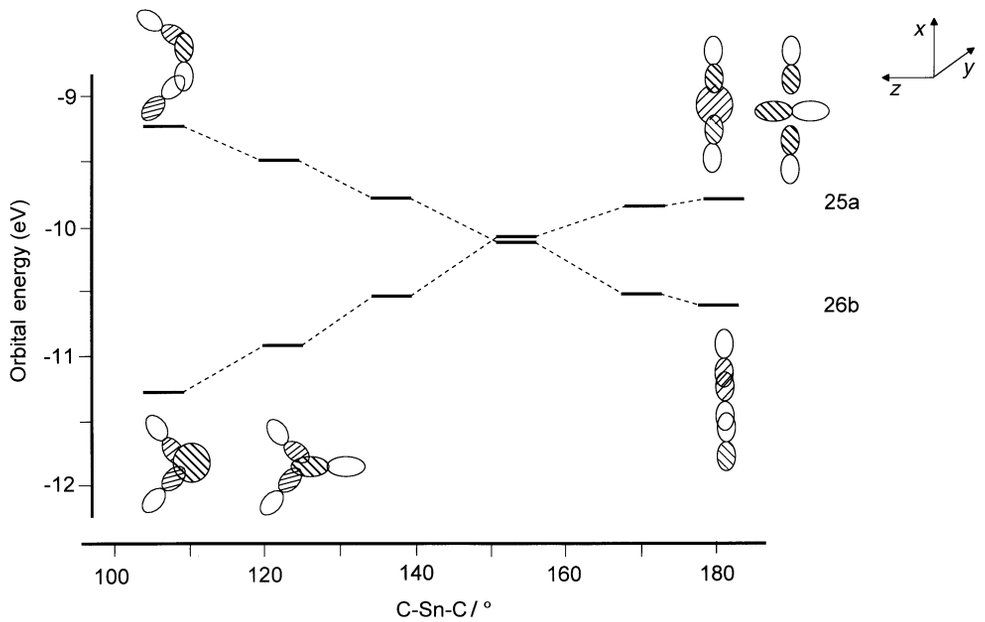


**Fig. 5** Variation of the calculated molecular orbitals energies of 26b and 25a with the $CH_3$–Sn–$CH_3$ bond angle in $Sn(CH_3)_2(trop)_2$

$Sn(CH_3)_2(dbzm)_2$ and $Sn(CH_3)_2(koj)_2$,*[14] where the Sn–C interactions are dominant; *cis* conformers prevail in the cases of $Sn(CH_3)_2(malt)_2$, $Sn(CH_3)_2(dhp)_2$ and $Sn(CH_3)_2(trop)_2$ due to the favoured $\sigma_{Sn-O}$ interactions.[14]

These considerations are consistent with previous results based on ligand–ligand repulsion models of several pseudo-octahedral $SnL_2$(chelate ligand)$_2$ complexes.[36] It has been shown that in the *cis* configuration the non-bonding interactions are minimized for all these classes of complexes. The *trans* geometries occurring in various dimethyl complexes have been, in addition, rationalized in terms of highly favoured σ interactions stabilizing the $Sn(CH_3)_2^{2+}$ cation.

## Conclusion

The relativistic effective-core-potential formalism has been successfully used to evaluate electronic and geometrical properties of $SnL_2(trop)_2$ complexes. They indicate *cis* equilibrium structures for both $SnCl_2(trop)_2$ and $Sn(CH_3)_2(trop)_2$ in agreement with X-ray structural data. In addition, they have provided a convincing rationale for the assignment of the PE spectra. Koopman's i.e. values are only slightly overestimated relative to the experimental data. The inclusion of relaxation effects through ΔSCF procedures has, however, provided a satisfactory fitting.

The Sn–L and Sn–trop bonds appear largely mediated by 5p and 5s metal orbitals interacting with $n_{\pm}(trop)$ and $\sigma_L$ ligand orbitals. The metal 4d orbitals provide a small, but not negligible, contribution. The total metal contribution to those MOs mainly responsible for both the Sn–L and Sn–trop bonding interactions has allowed a plausible rationale for (*i*) the preferred *cis* structures of the present complexes, (*ii*) the almost ubiquitous *cis* structures in chelate tin dihalide complexes and, finally, (*iii*) the possibility of stable *trans* conformations in the case of dimethyl complexes. The $\Delta E(\sigma_{Sn-L})$ orbital-energy separation strictly depends on the L–Sn–L bond angle (≈2 and ≈1 eV for *cis* and *trans* geometries, respectively). There is, therefore, evidence that gas-phase PE data can be diagnostic of the geometries involved.

* 2,3-Dihydroxypyridine, Hdhp; kojic acid (5-hydroxy-2-hydroxymethyl-4*H*-pyran-4-one), Hkoj; maltol (3-hydroxy-2-methyl-4*H*-pyran-4-one), Hmalt; dibenzoylmethane, Hdbzm.


## Acknowledgements

The authors gratefully thank the Ministero della Università e della Ricerca Scientifica e Tecnologica (MURST, Rome) and the Consiglio Nazionale delle Richerche (CNR, Rome) for their financial support. The CINECA computing centre (Casalecchio di Reno, Italy) is also gratefully acknowledged for a computer grant.


## References


1 M. M. McGrady and R. S. Tobias, *Inorg. Chem.*, 1964, **3**, 1157.
2 M. M. McGrady and R. S. Tobias, *J. Am. Chem. Soc.*, 1965, **87**, 1909.
3 R. Barbieri, G. Faraglia, M. Giustiniani and L. Roncucci, *J. Inorg. Nucl. Chem.*, 1964, **26**, 203.
4 L. Roncucci, G. Faraglia and R. Barbieri, *J. Organomet. Chem.*, 1964, **1**, 427.
5 W. H. Nelson and D. F. Martin, *J. Inorg. Nucl. Chem.*, 1965, **27**, 89.
6 T. Tanaka, M. Komura, Y. Kawasaky and R. Okawara, *J. Organomet. Chem.*, 1964, **1**, 484.
7 R. Ueda, Y. Kawasaki, T. Tanaka and R. Okawara, *J. Organomet. Chem.*, 1966, **5**, 194.
8 E. L Muetterties and C. M. Wright, *J. Am. Chem. Soc.*, 1964, **86**, 5132.
9 M. Komura, T. Tanaka and R. Okawara, *Inorg. Chim. Acta*, 1968, **2**, 321.
10 J. Otera, Y. Kawasaki and T. Tanaka, *Inorg. Chim. Acta*, 1967, **1**, 294.
11 J. A. Zubieta and J. J. Zuckerman, *Prog. Inorg. Chem.*, 1978, **24**, 251.
12 I. Waller, T. Halder, W. Schwarz and J. Weidlein, *J. Organomet. Chem.*, 1982, **232**, 99.
13 T. P. Lockhart and F. Davidson, *Organometallics*, 1987, **6**, 2471.
14 C. I. F. Denekamp, D. F. Evans, A. M. Z. Slawin, D. J. Williams, C. H. Y. Wong and J. D. Woollins, *J. Chem. Soc., Dalton Trans.*, 1992, 2375 and refs. therein.
15 G. A. Miller and E. O. Schlemper, *Inorg. Chem.*, 1973, **12**, 677.
16 S. H. Sage and R. S. Tobias, *Inorg. Nucl. Chem. Lett.*, 1968, **4**, 459.
17 T. P. Lockhart, W. F. Manders, E. O. Schlemper and J. J. Zuckerman, *J. Am. Chem. Soc.*, 1986, **108**, 4074.
18 R. W. Jones, jun. and R. C. Fay, *Inorg. Chem.*, 1973, **12**, 2599.
19 W. H. Nelson, *Inorg. Chem.*, 1967, **6**, 1509.
20 N. Serpone and K. A. Hersh, *Inorg. Chem.*, 1974, **13**, 2901; D. G. Bickley and N. Serpone, *Inorg. Chem.*, 1974, **13**, 2908.
21 J. Otera, T. Hinoishi, Y. Kawabe and R. Okawara, *Chem. Lett.*, 1981, 273.
22 J. Burgess and S. A. Parsons, *Polyhedron*, 1993, **12**, 1959.
23 W. F. Howard, jun., R. W. Crecely and W. H. Nelson, *Inorg. Chem.*, 1985, **24**, 2204.

24 R. B. Leblanc, jun. and W. H. Nelson, *J. Organomet. Chem.*, 1976, **113**, 257.
25 V. B. Ramos and R. S. Tobias, *Spectrochim. Acta, Part A*, 1973, **29**, 953.
26 V. B. Ramos and R. S. Tobias, *Spectrochim. Acta, Part A*, 1974, **30**, 181.
27 D. V. Naik, J. C. May and C. Curran, *J. Coord. Chem.*, 1973, **2**, 309.
28 B. W. Fitzsimmons, N. J. Seeley and A. W. Smith, *J. Chem. Soc. A*, 1969, 143.
29 T. K. Sham, J. S. Tse, V. Wellington and G. M. Bancroft, *Can. J. Chem.*, 1977, **55**, 3487.
30 G. M. Bancroft and T. K. Sham, *Can. J. Chem.*, 1974, **52**, 1361.
31 A. J. Rein and R. H. Herber, *J. Chem. Phys.*, 1975, **63**, 1021.
32 S. K. Brahma and W. H. Nelson, *Inorg. Chem.*, 1982, **21**, 4076.
33 W. H. Nelson and M. J. Aroney, *Inorg. Chem.*, 1973, **12**, 132.
34 C. Z. Moore and W. H. Nelson, *Inorg. Chem.*, 1968, **8**, 138.
35 J. W. Faller and A. Davidson, *Inorg. Chem.*, 1967, **6**, 182.
36 T. S. Tse, T. K. Sham and G. M. Bancroft, *Can. J. Chem.*, 1979, **57**, 2223; D. L. Kepert, *J. Organomet. Chem.*, 1976, **107**, 49; *Prog. Inorg. Chem.*, 1977, **23**, 1.
37 S. Di Bella, A. Gulino, G. Lanza, I. L. Fragalà and T. J. Marks, *Organometallics*, 1993, **12**, 3326.
38 W. R. Wadt and P. J. Hay, *J. Chem. Phys.*, 1985, **82**, 284.
39 W. J. Stevens, H. Basch and M. Krauss, *J. Chem. Phys.*, 1984, **81**, 6026.
40 W. J. Hehre, L. Radom, P. v. R. Schleyer and J. A. Pople, *Ab Initio Molecular Orbital Theory*, Wiley, New York, 1986.
41 M. Dupuis, A. Marquez and E. R. Davidson, HONDO 95.3 from CHEM-Station, IBM, Kingston, NY, 1995.
42 G. Bruno, G. Centineo, E. Ciliberto and I. Fragalà, *J. Electron Spectrosc. Relat. Phenom.*, 1983, **32**, 153.
43 I. Fragalà, E. Ciliberto, P. Finocchiaro and A. Recca, *J. Chem. Soc., Dalton Trans.*, 1979, 240.
44 R. Bertoncello, J. P. Daudey, G. Granozzi and U. Russo, *Organometallics*, 1986, **5**, 1866.
45 I. Fragalà, E. Ciliberto, R. G. Egdell and G. Granozzi, *J. Chem. Soc., Dalton Trans.*, 1980, 145.
46 J. J. Yeh and I. Lindau, *At. Data Nucl. Data Tables*, 1985, **32**, 1.
47 U. Gelius and K. Siegbahn, *Faraday Discuss. Chem. Soc.*, 1972, **54**, 257.
48 K. Kimura, S. Katsumata, Y. Achiba, T. Yamazaki and S. Iwata, *Handbook of He(I) Photoelectron Spectra*, Japan Scientific Societies Press, Tokyo, 1981.
49 S. Di Bella, G. Lanza, A. Gulino and I. Fragalà, *Inorg. Chem.*, 1996, **35**, 3885.

*Received* 3*rd September* 1996; *Paper* 6/06065J